NJC

Reversible and turn-on type fluorescence behaviour for hydrogen sulfide via redox cycle between selenoxide and selenide

Journal:	*New Journal of Chemistry*
Manuscript ID	NJ-ART-05-2019-002813.R1
Article Type:	Paper
Date Submitted by the Author:	21-Jun-2019
Complete List of Authors:	Annaka, Tatsuro; Saitama University, Department of Chemistry Nakata, Norio; Saitama Universtiy, Department of Chemistry Ishii, Akihiko; Saitama University, Department of Chemistry

ARTICLE

Reversible and turn-on type fluorescence behaviour for hydrogen sulfide via redox cycle between selenoxide and selenide†

6Received 00th January 20xx,
Accepted 00th January 20xx

DOI: 10.1039/x0xx00000x

Tatsuro Annaka, Norio Nakata and Akihiko Ishii *

A turn-on type fluorescence behaviour for H_2S based on a reversible selenoxide/selenide redox system is reported. Very weakly fluorescent selenoxides of 1,4-diphenyl-1-seleno-1,3-butadiene derivatives, incorporated with dibenzobarrelene (Dbb)- or (mono)benzobarrelene (Mbb) (DbbSeO and MbbSeO, respectively), are reduced quickly with NaSH as the equivalent of H_2S in a dilute solution of CH_3CN/PBS at pH 7.4 to yield the respective intensely fluorescent selenides (DbbSe and MbbSe). The selenoxides are highly selective for H_2S compared to other biothiols such as L-cysteine (Cys) and reduced gulthathione (GSH). On the other hand, the intense fluorescence of DbbSe is effectively quenched by oxidation with NaOCl as the equivalent of HOCl. The oxidation also showed high selectivity to HOCl against other oxidants such as H_2O_2, *t*-BuOOH, and $ONOO^-$. This reversibility of the fluorescence behaviour suggests that this system could monitor H_2S and HOCl generation in one-pot. The fluorescence properties of DbbSe and DbbSeO were discussed based on the results of TD-DFT calculations.

Introduction

Hydrogen sulfide (H_2S) is well known as the smell of rotten eggs and as a toxic gas. On the other hand, H_2S has been shown to be the third gas transmitter like nitric oxide and carbon monoxide.[1] H_2S is produced from enzymatic processes in mammalian organs and tissues, including relaxation of vascular smooth muscles, mediating neurotransmission, inhibition of insulin signalling, and regulation of inflammation and O_2 sensing.[2–6] Previous studies have shown that H_2S affects cardiovascular function, central nervous system and energy metabolism.[7] Abnormal levels of H_2S can cause disease such as gastric mucosal injury, liver cirrhosis and Alzheimer's disease.[8–10]

Current major detection methods for H_2S are colorimetric and electrochemical assays,[11] gas chromatography,[11] polarographic sensing[12] and nickel sulfide precipitation,[13] but these give variable results due to the rapid catabolism of H_2S. In contrast, fluorescence analysis offers advantages with high sensitivity, quantitativity and selectivity for in-situ observation. Recently, fluorescence probes for H_2S utilizing reactions such as azide reduction,[14,15] nucleophilic addition,[14,16] copper sulfide precipitation[17] and other reactions[18] have been reported. While these reaction-based probes demonstrate high detectability to H_2S with "turn-on" type fluorescence, they do not have reversibility to non-fluorescent starting materials.

Meanwhile, Han and co-workers have developed a reversible fluorescence redox system between H_2S and hypochlorous acid (HOCl) using the interconversion between BODIPY-based selenoxide and selenide (see below);[19] the intensely fluorescent selenoxide is reduced with H_2S to yield the weakly fluorescent selenide, which is oxidized with HOCl back to the intensely fluorescent selenoxide. Endogenous HOCl, one of reactive oxygen species (ROS),[20] has been reported to be essential for several biological functions.[21,22] However, excess HOCl is a major oxidative stress.[23] This reversible system is a turn-on system for HOCl, in other words, a "turn-off" system for H_2S.

We have previously reported the synthesis and photophysical properties of 1,2-bis(methoxycarbonyl)-1-seleno-1,3-butadiene derivative **1** and the selenoxide **2** which incorporate with dibenzobarrelene (Dbb).[24] **1** and **2** form a selenide-selenoxide redox cycle in the oxidation of **1** with *m*-chloroperoxybenzoic acid (MCPBA) and the reduction of **2** with PPh_3 (Scheme 1). Interestingly, the **1**/**2** system has characteristic fluorescence properties that are opposite to those of above-mentioned Han's selenide-selenoxide system[19]; selenide **1** shows intense fluorescence and selenoxide **2** does very weak fluorescence [**1**: $\Phi_F(CH_2Cl_2) = 0.86$; **2**: $\Phi_F(CH_2Cl_2) = 0.03$]. While the weak fluorescence of Han's selenide has been interpreted in light of intramolecular photoinduced electron-transfer (PET) and the

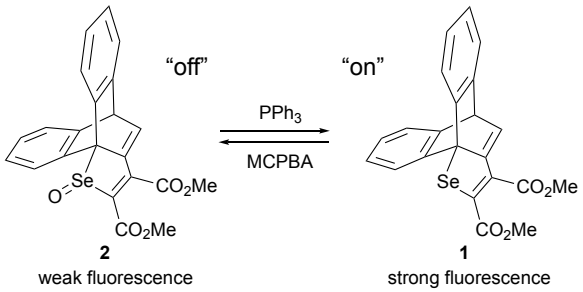

Scheme 1 Redox cycle between 1,2-di(methoxycarbonyl)-1-seleno-1,3-butadiene derivative **1** and its oxide **2**.

Department of Chemistry, Graduate School of Science and Engineering, Saitama University, 255 Shimo-okubo, Sakura-ku, Saitama, 338-8570, Japan.
E-mail: ishiiaki@chem.saitama-u.ac.jp

† Electronic Supplementary Information (ESI) available: ^1H and ^{13}C NMR charts, results of TD-DFT calculations, and ORTEPs and crystallographic data in CIF format of **5** and **6**. CCDC 1908243 (**5**) and 1908242 (**6**). For ESI and crystallographic data in CIF or other electronic formats see DOI: 10.1039/x0xx00000x

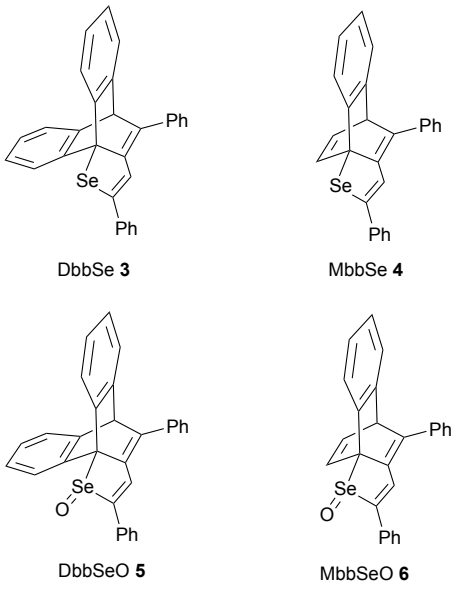

Chart 1

heavy atom effect,[19,25] selenide **1** is characterized by the intense fluorescence despite the presence of selenium, a heavy atom.[26] This redox system, however, has a few problems, low reactivity of **1** to oxidation due to the two electron-withdrawing methoxycarbonyl groups and instability of selenoxide **2**. After that, we also reported on 1,4-diphenyl-1-seleno-1,3-butadiene derivatives **3** and **4** incorporating Dbb and (mono)benzobarrelene (Mbb), respectively (Chart 1).[27] The selenides **3** and **4** show fluorescence with high efficiencies as well as **1**, and in contrast, the fluorescence efficiencies of the corresponding selenoxides **5** and **6** decrease as much as **2**. These fluorescence behaviours of **3**–**6** prompted us to investigate the possibility of using this selenide/selenoxide system as a fluorescence probe. As mentioned above, fluorescence probes for H_2S with reaction-based irreversible/turn-on systems and those that are redox-reversible/turn-off types have been reported so far.[28] Therefore, our system has the possibility to present the redox-reversible/turn-on type H_2S fluorescence probe, which has not been established yet as far as we know. It would be also important to add a new member to the library of traditional fluorophores used to study fluorescence sensors.

Here we report on the fluorescence behaviour of selenoxides **5** and **6** in the reduction with H_2S and other biothiols based on the dramatic changes of fluorescent intensity from **5** and **6** to selenides **3** and **4** (Scheme 2). In addition, as selenides **3** and **4** have the potential to serve as turn-off type fluorescence probes for oxidants, this possibility was also examined with some oxidants including HOCl. Hereafter, dibenzobarrelene-based selenide **3** and selenoxide **5** are abbreviated as DbbSe **3** and DbbSeO **5**, respectively, and similarly, (mono)benzobarrelene-based **4** and **6** as MbbSe **4** and MbbSeO **6**, respectively.

Results and discussion

Synthesis and Photophysical Properties of selenides DbbSe 3 and MbbSe 4 and selenoxides DbbSeO 5 and MbbSeO 6

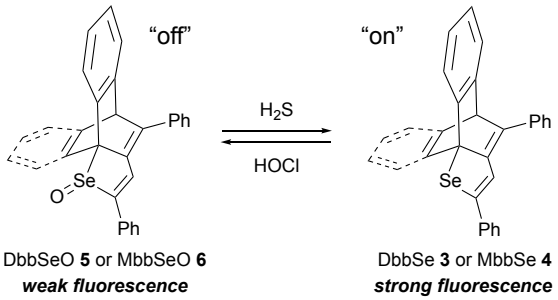

Scheme 2 Reversible fluorescence behaviour for H_2S/HOCl with dibenzobarrelene (Dbb)- and (mono)benzobarrelene (Mbb)-based selenides DbbSe **3** and MbbSe **4** and the respective selenoxides DbbSeO **5** and MbbSeO **6**.

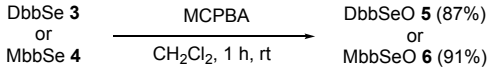

Scheme 3 MCPBA oxidation of DbbSe **3** or MbbSe **4** in CH_2Cl_2.

DbbSeO **5** and MbbSeO **6** were prepared by the oxidation of the respective DbbSe **3** and MbbSe **4**[27a] with MCPBA in high yields (Scheme 3). The structures of DbbSeO **5** and MbbSeO **6** were determined by spectroscopic methods and X-ray crystallography unambiguously (Figs. S1–S6, ESI†). The O atom in MbbSeO **6** was confirmed to be syn to the etheno bridge.

Photophysical data of **3**–**6** in CH_3CN and CH_3CN/H_2O (1:1) are summarized in Table 1. Their optical absorption and emission spectra in CH_3CN/H_2O (1/1) are shown in Fig. 1. Long-wavelength absorptions (λ_{abs} = 355, 359 nm) of DbbSeO **5** were blue-shifted by approximately 25 nm compared to those (λ_{abs} = 382, 383 nm) of DbbSe **3**. A similar tendency was observed between MbbSe **4** (λ_{abs} = 389, 389 nm) and MbbSeO **6** (λ_{abs} = 360, 364 nm). Their solvent effects on λ_{abs} are very small. The fluorescence maximum (λ_{em}) of DbbSeO **5** in CH_3CN/H_2O was observed at 480 nm, which is red-shifted by 23 nm compared to that in CH_3CN (λ_{em} = 457). This is probably due to hydrogen-bonding interactions between the selenoxide group and H_2O. DbbSe **3** undergoes almost no solvent effect. Similar tendencies were observed for MbbSeO **6** and MbbSe **4**. Fluorescence intensities of DbbSeO **5** and MbbSeO **6** were greatly reduced in each solvent as compared to those of DbbSe **3** and MbbSe **4**; in CH_3CN/H_2O under air, fluorescence quantum yields (Φ_F) of DbbSe **3** and DbbSe **4** are 0.89 and 0.86, respectively, and those of DbbSeO **5** and MbbSeO **6** were

Table 1 Photophysical data of DbbSe **3**, DbbSeO **5**, MbbSe **4** and MbbSeO **6**.[a]

Compound	Solvent	λ_{abs} (ε [b]) (nm)	λ_{em} (nm) [c]	Φ_F under Ar [d]	Φ_F under air [d]
DbbSe **3**	CH_3CN	382 (15300)	479	1.00	0.83
	CH_3CN/H_2O (1/1)	383 (15200)	480	– [e]	0.89
DbbSeO **5**	CH_3CN	355 (14800)	457	0.24	0.24
	CH_3CN/H_2O (1/1)	359 (16300)	480	– [e]	0.07
MbbSe **4**	CH_3CN	389 (15500)	485	1.00	0.74
	CH_3CN/H_2O (1/1)	389 (15600)	484	– [e]	0.86
MbbSeO **6**	CH_3CN	360 (22000)	451	0.007	0.006
	CH_3CN/H_2O (1/1)	364 (22100)	463	– [e]	0.006

[a] All solutions were adjusted at 1.0×10^{-5} M. [b] $M^{-1}\,cm^{-1}$. [c] Excited at respective absorption maxima. [d] Absolute fluorescence quantum yields were determined by using a calibrated integrating sphere system. [e] Not measured.

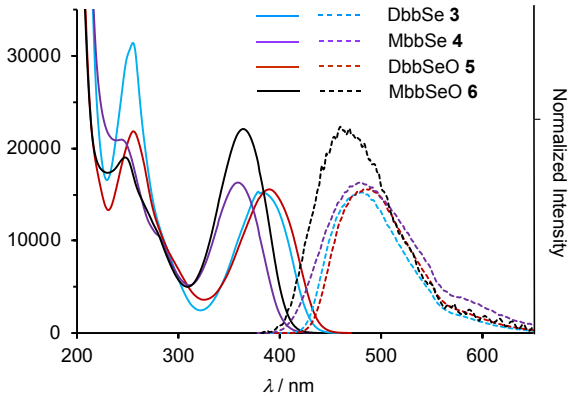

Fig. 1 Optical absorption (——) and fluorescence (----) spectra of **3**–**6** in CH_3CN/H_2O (50/50 v/v).

reduced to less than a tenth (Φ_F = 0.07) and a hundredth (Φ_F = 0.006), respectively.

Fluorescence properties of DbbSe **3** and DbbSeO **5** were considered, based on the account reported by Escudero for fluorescence quenching,[25c] with TD-DFT calculations. The lowest singlet transition ($S_0 \rightarrow S_1$, 3.16 eV) of DbbSe **3** is the HOMO-LUMO transition (100%) with an oscillator strength (*f*) of 0.365; the HOMO spreads over the π system mainly on the 1,4-diphenyl-1-seleno-1,3-butadiene (Se-C(Ph)=CH-C=C-Ph) moiety with a small contribution of the Dbb part (Fig. 2a), and the LUMO does mainly over the Se-C(Ph)=CH-C=C-Ph moiety with less contribution of the lone pair orbital on the selenium atom compared to that in HOMO. Thus, the transition is clearly assigned as a π-π* transition. The exited state of DbbSe **3** was optimized by TD-DFT (PBE0) calculations (Fig. 2b). In the optimized (relaxed) structure (S_1), although the torsion of two terminal phenyl groups with respect to the Se-C=CH-C=C plane become smaller, diagrams of (HOMO) and (LUMO) are basically similar to those of the S_0 state of **3**. The calculations showed that the lowest transition (2.20 eV) is mainly due to the (HOMO)-(LUMO) transition (96%) having π-π* character with a large *f* value of 0.449. There are no other singlet transitions like n-π* forbidden ones near this transition, indicating that the relaxed (S_1) state of DbbSe **3** is not a dark state[25c] that should have a very small *f* value near zero. This would be the reason for the intense fluorescence of **3** as observed.

The above calculations were also performed on DbbSeO **5**. In the optimized S_0 state, HOMO spreads mainly over the Ph-C=C-CH=C-Ph moiety with smaller contributions of the Dbb part and a lone pair orbital on the oxygen atom. In LUMO, the contribution of the Dbb part decreases considerably. HOMO–1 of **5** is the π– type of Se-O lone pairs, where the phases of the p-orbitals are opposite to one another. The lowest singlet transition (3.44 eV, *f* = 0.416) is a π-π* transition due to the HOMO-LUMO transition (100%). In the relaxed (S_1) state, diagrams of (HOMO–1), (HOMO), and (LUMO) resemble those of the S_0 state of **5**. The lowest singlet transition (2.29 eV) is a π-π* transition mainly due to the (HOMO)-(LUMO) transition (96%) with a large *f* value (0.498) as in the case of **3**, which is not consistent with the observed weak fluorescence (Φ_F = 0.24 in MeCN) compared to DbbSe **3**. Therefore, we should consider nonradiative pathways such

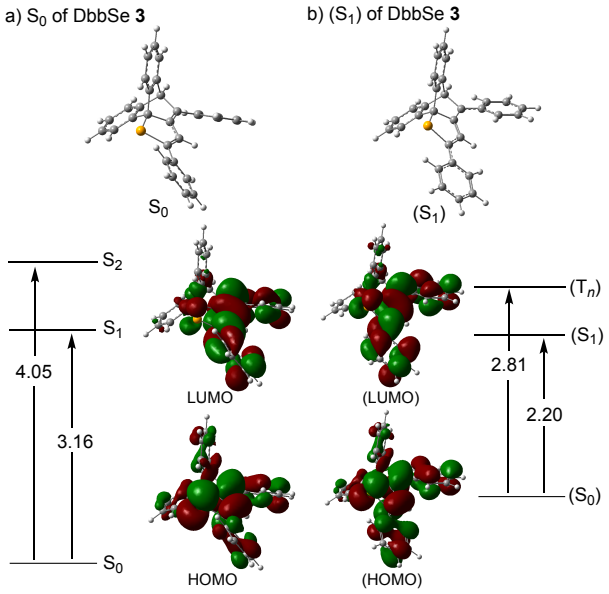

Fig. 2 (a) Optimized S_0 state structure of DbbSe **3**, diagrams of the frontier orbitals (HOMO and LUMO), and relevant transitions (eV) obtained by TD-DFT calculations. (b) Optimized S_1 state structure of DbbSe **3** [(S_1)], diagrams of the frontier orbitals [(HOMO) and (LUMO)] and relevant transitions (eV) obtained by TD-DFT calculations. TD-DFT calculations were performed at the PBE1PBE/6-31G(d) level.

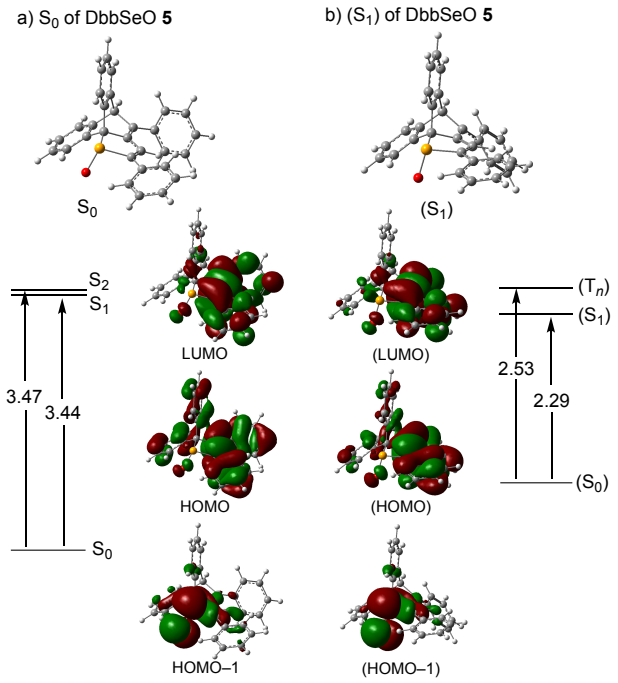

Fig. 3 (a) Optimized S_0 state structure of DbbSeO **5**, diagrams of the frontier orbitals (HOMO–1, HOMO and LUMO) and relevant transitions (eV) obtained by TD-DFT calculations. (b) Optimized S_1 state structure of DbbSeO **5** [(S_1)], diagrams of the frontier orbitals [(HOMO–1), (HOMO) and (LUMO)] and relevant transitions (eV) obtained by TD-DFT calculations. TD-DFT calculations were performed at the PBE1PBE/6-31G(d) level.

as the conical intersection between the S_2 and S_1 states and/or the intersystem crossing (ISC) between the relaxed (S_1) state and an energetically appropriate triplet state (T_n); Escudero has succeeded in the explanation of the low fluorescence quantum yield of butyl(9-anthrylmethyl)amine by the ultrafast conical intersection between S_1 and S_2 states with ADC(2) and CASPT2 calculations, where the calculated energy difference between the two states was 0.28 eV (ADC(2)).[25c] The above TD-DFT calculations for DbbSeO **5** showed the presence of the S_2 state (3.47 eV, f = 0.0010) only 0.04 eV above the S_1 state at the Frank-Condon region; in the case of DbbSe **3**, the S_2 state is above 0.89 eV of the S1 state. The S_0-S_2 transition is due to the HOMO–1-LUMO transition (100%) and assigned as an n-π* transition with a small f value. Therefore, the conical intersection appears to be a possible pathway for the fluorescence decrease of DbbSeO **5**. An alternative possibility is ISC. The TD-DFT optimization calculations on **5** shows the presence of a triplet state (2.54 eV, f = 0.00) above 0.24 eV of the relaxed (S_1) state, which is considerably small compared to 0.61 eV for the case of DbbSe **3**. The triplet transition for **5** is related to (HOMO–1) and (LUMO) (100%). This small energy difference may make ISC possible. Thus, the low fluorescence quantum yield of DbbSeO **5** is considered to be due to the conical intersection between the S_1 and S_2 states and/or ISC from the relaxed (S_1) state to a triplet state.

Fluorescence in CH_3CN/H_2O. Because compounds **3**–**6** are sparsely soluble in water, we optimized the proportion of the mixed

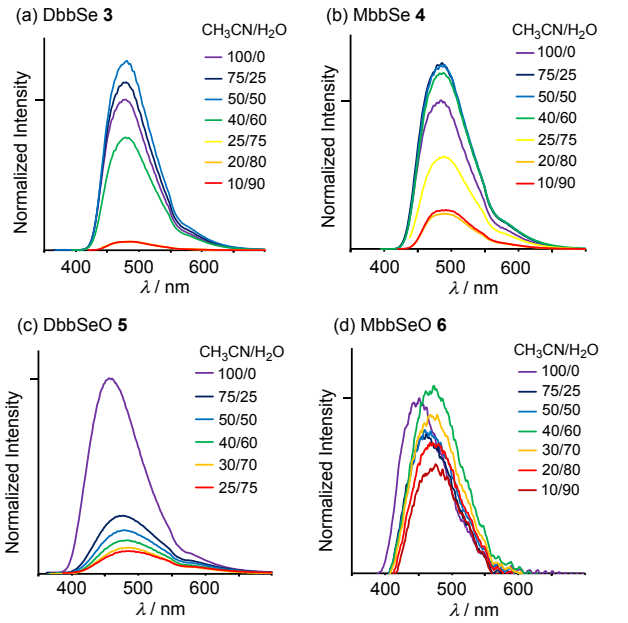

Fig. 4 Fluorescence spectra of (a) DbbSe **3**, (b) MbbSe **4**, (c) DbbSeO **5**, and (d) MbbSeO **6** in CH_3CN/H_2O (1.0×10^{-5} M) with ratios from 100/0 to 10/90 v/v.

solvent of CH_3CN and H_2O. When the ratio of H_2O increased, the fluorescence intensities of DbbSe **3** and MbbSe **4** were gradually enhanced until the ratio reached 50% v/v. Further increasing the ratio of H_2O decreased the fluorescence intensity due to precipitation (Figs. 4a and 4b, respectively). In contrast, the fluorescence intensities of DbbSeO **5** and MbbSeO **6** decreased gradually with the increase of the ratio of H_2O (Figs. 4c and 4d, respectively). Thus, we set the ratio of CH_3CN/H_2O as 50/50 v/v for following experiments to bring about the largest difference in fluorescence intensity for the of **3**/**5** and **4**/**6** pairs.

Sensing Abilities

Reduction of DbbSeO 5 and MbbSeO 6 with H_2S, Cys and GSH. First, the efficiency of the reduction of DbbSeO **5** with H_2S in a dilute solution was investigated. NaSH in phosphate buffer saline (PBS, pH 7.4) was employed as the equivalent of H_2S, and the NaSH is hereafter referred to as H_2S. The reaction of DbbSeO **5** with 2 molar equivalents of H_2S in CH_3CN/PBS occurred rapidly, and the reaction mixture exhibited strong fluorescence immediately after the addition of H_2S. The reduction completed within 30 min, and the ^1H NMR analysis of the reaction mixture showed quantitative formation of DbbSe **3** (Table 2). The reduction with an equimolar amount of H_2S was slow; the yield after 30 min was 60%. MbbSeO **6** was also quantitatively reduced with 2 molar equivalents of H_2S. Next, we investigated the reduction of DbbSeO **5** and MbbSeO **6** with other biothiols, L-cysteine (Cys) and reduced gulthathione (GSH). As shown in Table 2, Cys and GSH showed low efficiencies compared to H_2S; the reductions with 2 molar equivalents of Cys or GSH for 30 min at room temperature were slow and incomplete.

The reactivity of the three reductants appears to decrease as the bulkiness around the sulfur atom increases in the order of H_2S < Cys

Table 2 Reduction of DbbSeO **5** and MbbSeO **6** to DbbSe **3** and MbbSe **4** with 2 molar equivs of H_2S,[a] L-cysteine (Cys), or reduced gulthathione (GSH) in CH_3CN/PBS.[b]

Selenoxide	Reductant	Yield (%) [c]
DbbSeO **5**	NaSH	100
	Cys	36
	GSH	8
MbbSeO **6**	NaSH	100
	Cys	54
	GSH	18

[a] A solution of NaSH in PBS. [b] In a 2.3×10^{-4} M solution of a mixed solvent of 50/50 v/v CH_3CN/PBS (pH 7.4) for 30 min at room temperature. [c] Determined by ^1H NMR of the reaction mixture.

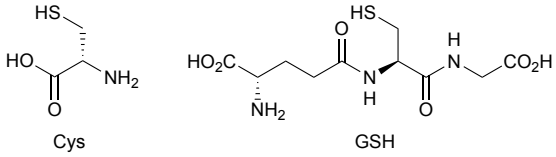

< GSH. Furthermore, in the case of Cys and GSH, the yields are higher for MbbSeO **6** than more sterically crowded DbbSeO **5**. These observations suggest that this reduction is sensitive to the steric hindrance between the selenoxide groups in **5** and **6** and the sulfur groups in reductants in the transition states. Another factor for the low reactivity of Cys and GSH seems to be related to pK_a values of their SH groups;[29] H_2S 7.0, Cys 8.3, and GSH 9.0.[30] The molar fractions of the ionized forms (RS^-) of Cys and GSH under the buffered conditions (pH 7.4) are much less than half based on the Henderson-Hasselbalch equation, which are in stark contrast to that for H_2S being estimated to be greater than half. With respect to the reaction mechanism of the reduction of selenoxides with thiols, hypervalent oxy(thio)selenuranes have been proposed as the intermediates to further react with thiols to form selenides, disulfides and H_2O.[31–34] Scheme 4 shows a plausible reaction mechanism for the reduction of DbbSeO **5** and MbbSeO **6** with thiols based on the above discussion and previous papers[31–34]. The attack of RS^-/RSH at the selenoxide selenium atom forms oxy(thio)selenurane intermediate **7**, which has RS and OH groups at the apical positions that suffer steric hindrance from Dbb or Mbb frameworks to make this step rate-controlling.[32] As the steric hindrance in Dbb **7** is greater than that in Mbb **7**, the transition state energy to Dbb **7** would be greatly influenced by the

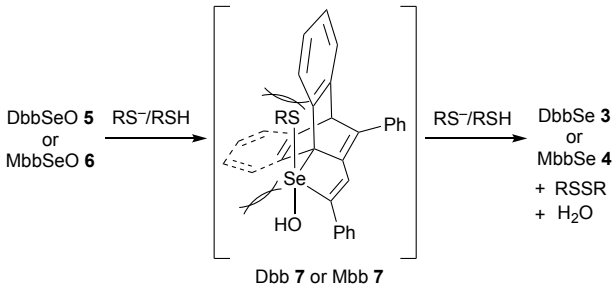

Scheme 4 A plausible mechanism of the reduction of selenoxides DbbSeO **5** and MbbSeO **6** with RS^-/RSH.

steric bulkiness of thiolates compared to that to Mbb **7** to lead to a relatively high selectivity of DbbSeO **5** to reductants. Subsequently, the nucleophilic attack of another RS^-/RSH on the RS group in **7** gives rise to selenides DbbSe **3** or MbbSe **4** together with disulfide (RSSR) and H_2O.[31–34] In the case of H_2S, disulfane (HSSH) should form. Disulfane is known to tend to decompose into H_2S and 1/8 S_8.[35] The regeneration of H_2S would cause the reduction yield to exceed 50% (60%) when only an equimolar amount of H_2S was used (see above).

The reduction of DbbSeO **5** and MbbSeO **6** with H_2S was performed in a more dilute solution. The reaction was monitored by optical absorption and fluorescence spectroscopies. As shown in Fig. 3, when 1 to 6 equivalents of solutions of H_2S (9–54×10^{-5} M) were added to an equal volume of a solution of **5** in CH_3CN (9.08×10^{-5} M), the absorption due to DbbSe **3** was observed at λ_{abs} = 383 nm in optical absorption spectra (Fig. 5a). An isosbestic point was observed at 376 nm indicating that the reduction proceeded cleanly. In the fluorescence spectra, the emission due to DbbSe **3** was observed at λ_{em} = 480 nm, and the intensities were enhanced as the equivalent of H_2S was increased (Fig. 5b). A quite similar behaviour was observed for MbbSeO **6** (Fig. 4); in the optical absorption spectra, the isosbestic point was observed at 386 nm (Fig. 6a). Bright blue fluorescences due to DbbSe **3** and MbbSe **4** were observed with the naked eye. Figure 7 exhibits time profiles of fluorescence intensity;

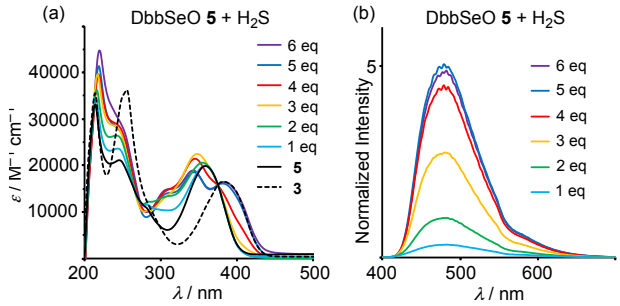

Fig. 5 (a) Optical absorption and (b) fluorescence (λ_{ex} = 383 nm) spectra after 30 min from additions of 1–6 equivs of H_2S (NaSH in PBS) (9–54×10^{-5} M) to a solution of DbbSeO **5** in CH_3CN (9.08×10^{-5} M).

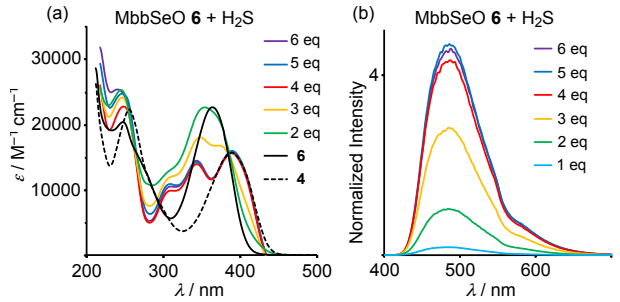

Fig. 6 (a) Optical absorption and (b) fluorescence (λ_{ex} = 389 nm) (b) spectra after 30 min from additions of 1–6 molar equivs of H_2S (NaSH in PBS) (9–54×10^{-5} M) to a solution of MbbSeO **6** in CH_3CN (9.08×10^{-5} M).

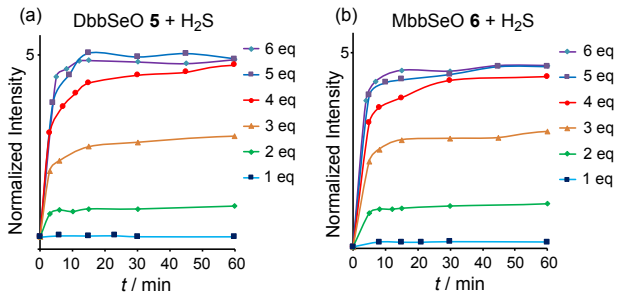

Fig. 7 Time profiles of fluorescent intensity. (a) In the reaction of DbbSeO **5** (4.5×10^{-5} M) with 1–6 molar equivs of H_2S in CH_3CN/PBS (50/50 v/v) and (b) in the reaction of MbbSeO **6** (4.5×10^{-5} M) in with 1–6 molar equivs of H_2S in CH_3CN/PBS (50/50 v/v).

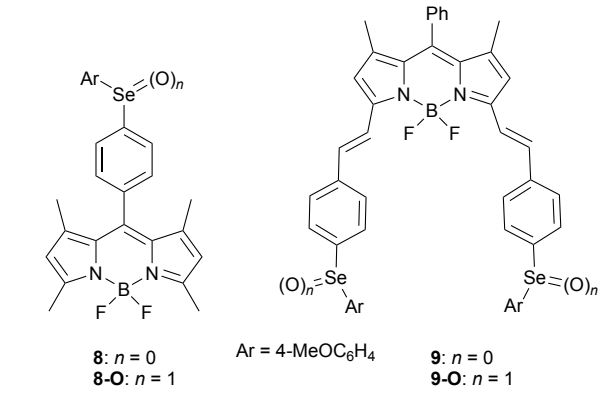

8: $n = 0$
8-O: $n = 1$

Ar = 4-$MeOC_6H_4$

9: $n = 0$
9-O: $n = 1$

Chart 2

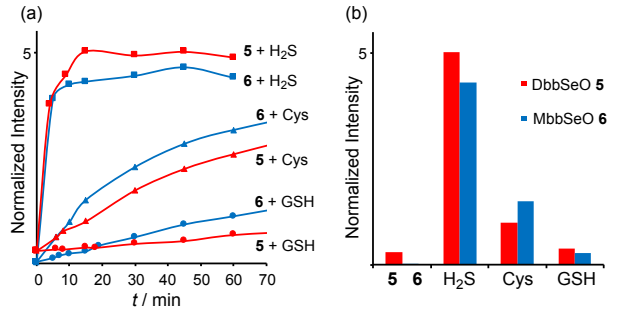

Fig. 8 (a) Time profiles of fluorescent intensity at 480 nm in the reactions of DbbSeO **5** (red) or MbbSeO **6** (blue) in CH_3CN (9.08×10^{-5} M) with 5 molar equivs of H_2S (■), Cys (▲), or GSH (●) in PBS (45×10^{-5} M). (b) Comparison of the fluorescence intensity of **5** (red) and **6** (blue) after 15 min from additions of the reductants.

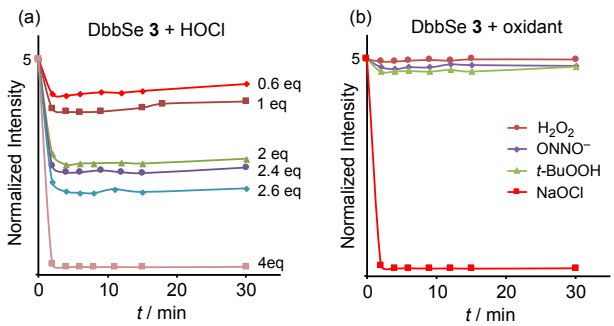

Fig. 9 Time profiles of fluorescence intensity at 480 nm (a) in the reactions of DbbSe **3** (5.0×10^{-5} M) with 0.6–10 molar equivs of HOCl in CH_3CN/PBS (50/50 v/v) and (b) in the reactions of DbbSe **3** (5.0×10^{-5} M) with 4 molar equivs of HOCl (■), H_2O_2 (●), *t*-BuOOH (▲), or $ONOO^-$ (◆) in CH_3CN/PBS (50/50 v/v).

the fluorescence intensity reached a constant after around 15 min with any equivalents of H_2S, and 4–5 equivalents of H_2S are necessary to complete the reduction.

The reductions of DbbSeO **5** and MbbSeO **6** with 5 molar equivalents of Cys and GSH were investigated under similar conditions. Figure 8a depicts the time profiles of the increase in fluorescence intensity at 480 nm together with those of H_2S. As expected from the results shown in Table 2, the reductions with Cys and GSH were much slower than that with H_2S. In addition, DbbSeO **5** showed somewhat higher selectivity between H_2S and others (Cys and GSH) in the early stage of the reaction compared to MbbSeO **6**. Figure 8b shows a comparison of fluorescence intensities after 15 min.

According to the report from Han's group, the reduction of fluorescent selenoxide **8-O** at 1×10^{-5} M with 10 molar equivalents of H_2S in CH_3CN/PBS (30/70 v/v) was completed within 5 min to give selenide **8** (Chart 2).[19a] Under similar conditions, fluorescent bis(selenoxide) **9-O** was reduced with H_2S in CH_3CN/PBS (20/80 v/v) to give bis(selenide) **9** within 10 min.[19c] Both **8-O** and **9-O** show high selectivity for H_2S against other reductants.[19a,c] Thus, the above results show that the reactivities of selenoxide **5** and **6** toward H_2S are comparable to those of **8-O** and **9-O**.

Oxidation of DbbSe 3 with HOCl, H_2O_2, *t*-BuOOH, and $ONOO^-$. The oxidation of DbbSe **3** with HOCl, H_2O_2, *t*-BuOOH and $ONOO^-$ in CH_3CN/PBS (50/50 v/v) was examined. NaOCl in PBS was used as an equivalent of HOCl, and the NaOCl in PBS is referred to as HOCl hereafter. When **3** was treated with 4 molar equivalents of HOCl, the oxidation completed in a few minutes, and the fluorescence due to DbbSe **3** was completely quenched (Fig. 9a). On the other hand, the reaction mixture treated with 4 equivalents of H_2O_2, *t*-BuOOH or $ONOO^-$ continued to emit intensely even after 30 min (Fig. 9b), indicating that DbbSe **3** has better selectivity to HOCl among the examined oxidants. The reactivity of **3** toward oxidants is also comparable to those of selenides **8** and **9** (Chart 2) that showed high selectivity for HOCl or HOBr, respectively, against other oxidants; the oxidation of **8** (1×10^{-5} M, CH_3CN/PBS 30/70 v/v) with 5 molar equivalents of HOCl was completed within 20 min to give **8-O**, and that of **9** with 10 molar equivalents of HOBr under similar conditions (CH_3CN/PBS 20/80 v/v) finished in 5 min.[19a,c]

Finally, the cycle of reduction-oxidation of DbbSeO **5** in one pot was investigated. DbbSeO **5** was reduced to DbbSe **3** with 5 equivalents of H_2S, and then HOCl were added. As shown in Fig. 10, more than 10 equivalents of HOCl were required to decrease the

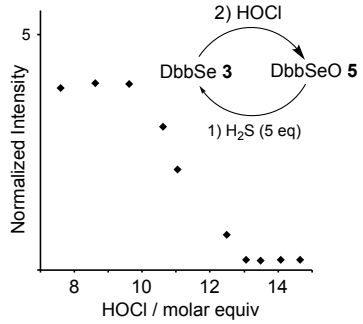

Fig. 10 Fluorescence response at 480 nm after 15 min from additions of 7.5–14.5 molar equivs of HOCl (NaOCl in PBS) to a solution of DbbSeO **5** (5.0×10^{-5} M) pre-treated with 5 molar equivs of H_2S in CH_3CN/PBS (50/50 v/v).

fluorescence from DbbSe **3** to preferentially reduce the excess H_2S used in the previous step. The fluorescence was quenched almost completely when 13 and more equivalents of HOCl were treated. Although an excess amount of HOCl was necessary to quench the fluorescence from DbbSe **3** under the present conditions, this result suggests the potential of DbbSe **3**/DbbSeO **5** applied as a probe to monitor the redox cycle between H_2S reduction and HOCl oxidation.

Conclusions

We reported redox-reversible/turn-on type fluorescence behaviour for H_2S utilizing the interconversion between 1,4-diphenyl-1-seleno-1,3-butadiene derivatives DbbSe **3** and MbbSe **4** and the respective selenoxides DbbSeO **5** and DbbSeO **6**. This system presents a probe complementary to Han's redox-reversible/turn-off type fluorescence probes for H_2S. DbbSeO **5** and MbbSeO **6** can detect H_2S more sensitively, quantitatively and selectively than Cys and GSH. When DbbSeO **5** and MbbSeO **6** are compared, **5** shows higher selectivity for reductants than **6**, which seems to be due to steric repulsion between the bulky dibenzobarrelene skeleton in **5** and the reductants. The oxidation of DbbSe **3** with HOCl takes place immediately, quantitatively and selectively as compared to other oxidants examined. Thus, DbbSeO **5**/DbbSe **3** has the potential to be applied as a fluorescent probe to monitor the redox cycle between H_2S reduction and HOCl oxidation under simulated physiological conditions. TD-DFT calculations suggested the effective radiative pathway for DbbSeO **3** and the presence of nonradiative pathways for DbbSeO **5**.

Experimental

General Procedure

All melting points were determined on a Mel-Temp capillary tube apparatus and were uncorrected. ^{1}H, ^{13}C and ^{77}Se NMR spectra were recorded on AVANCE-400 (400 MHz for ^{1}H and 101 MHz for ^{13}C) and AVANCE-500T (95.4 MHz for ^{77}Se) spectrometers using $CDCl_3$ as the solvent at room temperature. IR spectra were recorded on a Perkin Elmer System 2000 FT-IR spectrometer. UV-vis spectra were recorded on a JASCO V-560 spectrophotometer. Fluorescence spectra were recorded on a JASCO FP-6300 spectrofluorometer. Absolute photoluminescence quantum yields were measured by a calibrated integrating sphere system C10027 (Hamamatsu Photonics). LC-ESI-MS data were obtained by using a Hitachi NanoFrontier eLD. Elemental analyses were carried out at the Molecular Analysis and Life Science Center of Saitama University. X-ray crystallography was performed with a Bruker AXS SMART diffractometer. The intensity data were collected at 100 K employing graphite-monochromated MoKα radiation (λ = 0.71073 Å) and the structures were solved by direct methods and refined by full-matrix least-squares procedures on F^2 for all reflections (SHELX-97).[36] Solvents were dried by standard methods and freshly distilled prior to use. Phosphate buffer saline (PBS, 1×10^{-2} M, pH 7.4) was purchased from Wako Pure Chemical Industries, Ltd.

2,4-Diphenyl-5*H*-5,9b[1',2']-benzenonaphtho[1,2-*b*]selenophene 1-Oxide (5)

A mixture of DbbSe **3** (60 mg, 0.13 mmol) and MCPBA (95%) (36 mg, 0.20 mmol) was dissolved in CH_2Cl_2 (5 mL), and the mixture was stirred for 1 h. The reaction was stopped by addition of aqueous Na_2SO_3 and then aqueous $NaHCO_3$, and the mixture was extracted with CH_2Cl_2. The extract was washed with water and dried over anhydrous Na_2SO_4. After removal of the solvent under reduced pressure, the residue was purified by reprecipitation from a CH_2Cl_2/hexane solution to give DbbSeO **5** (54 mg, 87%): Pale yellow crystals, mp 192–193 °C decomp (hexane/$CHCl_3$). ^{1}H NMR (400 MHz) δ 5.41 (s, 1H), 7.03–7.16 (m, 4H), 7.34–7.47 (m, 11H), 7.63–7.67 (m, 1H), 7.73–7.77 (m, 2H), 8.89 (dd, J = 7, 1 Hz, 1H); ^{13}C{^{1}H} NMR (101 MHz, $CDCl_3$) δ 57.0 (CH), 73.2 (C), 122.4 (CH), 123.2 (2CH), 123.4 (CH), 125.3 (CH), 125.4 (CH), 125.5 (CH), 126.6 (CH), 127.1 (2CH), 127.2 (2CH), 128.7 (CH), 128.9 (2CH), 129.2 (2CH+CH), 129.5 (CH), 133.1 (C), 137.1 (C), 142.9 (2C), 143.1 (C), 147.3 (C), 148.3 (C), 150.4 (C), 150.9 (C) (2CH: two equivalent *o*- or *m*-CH carbons of phenyl groups or two overlapped CH carbons); ^{77}Se{^{1}H} NMR (95.4 MHz, $CDCl_3$) δ 992.2; IR (KBr) $\tilde{\nu}$ 818 cm^{-1} (Se=O). Found: C, 75.61; H, 4.15%. Anal. Calcd. for $C_{30}H_{20}OSe$: C, 75.79; H, 4.24%.

2,4-Diphenyl-5*H*-5,9b[1',2']-ethenonaphtho[1,2-*b*]selenophene 1-Oxide (6)

A mixture of MbbSe **4** (511 mg, 1.25 mmol) and MCPBA (95%) (340 mg, 1.87 mmol) was dissolved in CH_2Cl_2 (20 mL), and the mixture was stirred for 1 h. To the mixture were added aqueous Na_2SO_3 and aqueous $NaHCO_3$, and the mixture was extracted with CH_2Cl_2. The extract was washed with water and dried over anhydrous Na_2SO_4. After removal of the solvent under reduced pressure, the residue was purified by reprecipitation from a CH_2Cl_2/hexane solution to give MbbSeO **6** (483 mg, 91%): Orange crystals, mp 195–197 °C decomp (hexane/$CHCl_3$). ^{1}H NMR (400 MHz) δ 5.35 (dd, J = 6, 1 Hz, 1H), 7.02–7.13 (m, 2H), 7.15 (dd, J = 7, 6 Hz, 1H), 7.32–7.46 (m, 11H), 7.56 (dd, J = 7, 1 Hz, 1H), 7.72–7.77 (m, 2H); ^{13}C{^{1}H} NMR (101 MHz, $CDCl_3$) δ 55.6 (CH), 77.2 (C), 121.4 (CH), 122.8 (CH), 124.7 (CH), 125.9 (CH), 126.92 (2CH), 126.94 (2CH), 128.5 (CH), 128.9 (2CH), 129.2 (2CH), 129.3 (CH), 129.5 (CH), 133.3 (CH), 133.4 (C), 137.2 (C), 138.1 (CH), 143.1 (C), 147.2 (C), 149.0 (C), 151.2 (C), 151.7 (C) (2CH: two equivalent *o*- or *m*-CH carbons of phenyl groups) ; ^{77}Se{^{1}H} NMR (95.4 MHz, $CDCl_3$) δ 933.5; IR (KBr) $\tilde{\nu}$ 817 cm^{-1} (Se=O). HRMS (ESI) Calcd. for $C_{26}H_{18}OSe\cdot H$: M = 427.05956. Found 427.06342 (M^++H^+).

Crystallographic data

DbbSeO **5** (CCDC-1908243†): $C_{30}H_{20}OSe•2(CHCl_3)$, M_W = 714.16, triclinic, space group *P*–1, *Z* = 2, *a* = 10.3946(6), *b* = 11.3394(7), *c* = 12.8696(8) Å, α = 90.7040(10)°, β = 98.331(2)°, γ = 92.8220(10)°, *V* = 1498.80(16) Å^3, $D_{calcd.}$ = 1.582 g cm^{-3}, R_1 [$I > 2\sigma(I)$] = 0.0463, wR_2 (all data) = 0.1196 for 6817 reflections, 361 parameters and GOF = 1.011.

MbbSeO **6** (CCDC-1908242†): $C_{26}H_{18}OSe•O$, M_W = 441.36, monoclinic, space group $P2_1$, *Z* = 2, *a* = 0.1234(6), *b* = 12.7495(8), *c* = 9.6022(6) Å, β = 116.3210(10)°, *V* = 1001.12(11) Å^3, $D_{calcd.}$ = 1.464 g cm^{-3}, R_1 [$I > 2\sigma(I)$] = 0.0330, wR_2 (all data) = 0.0745 for 3626 reflections, 262 parameters, 1 restraint and GOF = 1.038.

Reduction of DbbSeO 5 and MbbSeO 6 with RSH

Typical procedure for ^{1}NMR measurement. Reduction of DbbSeO 5 with NaSH in CH_3CN/PBS (50/50 v/v) (Table 2).

A solution of DbbSeO **5** in CH_3CN (9.25×10^{-3} M) was diluted with 19 mL of CH_3CN and 19 mL of PBS. To the solution, 1 mL of a solution of NaSH in PBS (2.03×10^{-2} M) was added. The mixture was stirred for 30 min at room temperature, and then diluted with ethyl acetate. The organic layer was separated, washed with brine, dried over anhydrous Na_2SO_4 and evaporated to dryness. The ^{1}H NMR spectrum of the residue showed the quantitative formation of DbbSe **3**.

In a similar manner, the reactions of other runs in Table 2 were carried out. The concentration of a solution of NaSH in PBS was determined before use by iodometric titration; to 10 mL of an aqueous solution of I_2/KI (2.02×10^{-2} M) was added a 5 mL of a solution of NaSH in PBS. Under stirring, an aqueous solution of $Na_2S_2O_3$ (1.99×10^{-2} M) was added dropwise to turn the colour of the solution from brown to colourless. It required 9.9 mL of the solution of $Na_2S_2O_3$ to determine the concentration of the PBS solution of NaSH as 2.03×10^{-2} M.

Procedure for optical absorption and fluorescence measurements. Reduction of DbbSeO 5 with NaSH in CH_3CN/PBS (50/50 v/v)

5 mL of a solution of DbbSeO 5 in CH_3CN (9.08×10^{-5} M) and 5 mL of a respective concentration of a solution of NaSH in PBS were mixed. The mixture was shaken vigorously, stood for 30 min, and then subjected to optical absorption and fluorescence measurements.

Oxidation of DbbSe 3 for fluorescence measurement

The concentrations of aqueous solutions of NaOCl and H_2O_2 were determined before use by iodometric titration; I_2 formed by the reaction of KI with NaOCl or H_2O_2 in the presence of sulfuric acid was titrated with an aqueous solution of $Na_2S_2O_3$. PBS solutions of NaOCl and H_2O_2 were then prepared with the respective aqueous solutions. A solution of $ONOO^-$ was prepared by mixing a PBS solution of H_2O_2 and 1.1 equivs of isoamyl nitrite and NaOH.[37]

Typical procedure: 2.5 mL of a solution of DbbSeO **5** in CH_3CN (9.92×10^{-5} M) and 2.5 mL of a respective concentration of a solution of an oxidant in PBS were mixed. The mixture was shaken vigorously, stood for each time, and then subjected to fluorescence measurement.

Computational details

All calculations were performed on the Gaussian 09 program.[38] The PBE0 method[39,40] was used as the DFT functional, which was employed for the evaluation of the dark-state mechanism for fluorescence quenching.[25c] Initial structures of DbbSe **3** and DbbSeO **5** were taken from their structures obtained by X-ray crystallography. Their ground states were optimized at the PBE1PBE/6-31G(d) level, followed by TD-DFT calculation at the same level. Their excited states were optimized at the PBE1PB1/6-31G(d) level with the TD and OPT keywords; the initial structures were taken from the respective triplet state structures optimized from their optimized ground states structures.

Conflicts of interest

There are no conflicts to declare.

Acknowledgements

T. A. acknowledges the Japan Society for the Promotion of Science (JSPS) for a fellowship for young scientists. N. N. thanks a financial support by Adaptable and Seamless Technology Transfer Program through Target-driven R&D (A-STEP) from Japan Science and Technology Agency (JST) (2015).

References

1 (a) E. Łowicka, J. Beltowski, *Pharmacol. Rep.*, 2007, **59**, 4; (b) M. Lavu, S. Bhushan, D. J. Lefer, *J. Clin. Sci.*, 2011, **120**, 219; (c) M. Whiteman, P. K. Moore, *J. Cell. Mol. Med.*, 2009, **13**, 488.
2 G. Yang, L. Wu, B. Jiang, W. Yang, J. Qi, K. Cao, Q. Meng, A. K. Mustafa, W. Mu, S. Zhang, S. H. Snyder, R. Wang, *Science*, 2008, **322**, 587.
3 K. Abe, H. Kimura, *J. Neurosci.*, 1996, **16**, 1066.
4 (a) Y. Kaneko, Y. Kimura, H. Kimura, I. Niki, *Diabetes*, 2006, **55**, 1391; (b) W. Yang, G. Yang, X. Jia, L. Wu, R. Wang, *J. Physiol.*, 2005, **569**, 519.
5 (a) L. Li, M. Bhatia, Y. Z. Zhu, Y. C. Zhu, R. D. Ramnath, Z. J. Wang, F. B. M. Anuar, M. Whiteman, M. Salto-Tellez, P. K. Moore, *FASEB J.*, 2005, **19**, 1196; (b) R. C. O. Zanardo, V. Brancaleone, E. Distrutti, S. Fiorucci, G. Cirino, J. L. Wallace, *FASEB J.*, 2006, **20**, 2118.
6 Y.-J. Peng, J. Nanduri, G. Raghuraman, D. Souvannakitti, M. M. Gadalla, G. K. Kumar, S. H. Snyder, N. R. Prabhakar, *Proc. Natl. Acad. Sci. U.S.A.*, 2010, **107**, 10719.
7 For a review, see O. Kabil, R. Banerjee, *J. Biol. Chem.*, 2010, **285**, 21903.
8 S. Fiorucci, E. Antonelli, E. Distrutti, G. Rizzo, A. Mencarelli, S. Orlandi, R. Zanardo, B. Renga, M. D. Sante, A. Morelli, G. Cirino, J. L. Wallace, *Gastroenterology*, 2005, **129**, 1210.
9 S. Fiorucci, E. Antonelli, A. Mencarelli, S. Orlandi, B. Renga, G. Rizzo, E. Distrutti, V. Shah, A. Morelli, *Hepatology*, 2005, **42**, 539.
10 (a) K. Eto, T. Asada, K. Arima, T. Makifuchi, H. Kimura, *Biochem. Biophys. Res. Commun.*, 2002, **293**, 1485; for a review, see (b) K. Qu, S. W. Lee, J. S. Bian, C.-M. Low, P. T.-H. Wong, *Neurochem. Int.*, 2008, **52**, 155.
11 For reviews, (a) T. Ubuka, *J. Chromatogr. B.*, 2002, **781**, 227; (b) A. Tangerman, *J. Chromatogr. B*, 2009, **877**, 3366.
12 J. E. Doeller, T. S. Isbell, G. Benavides, J. Koenitzer, H. Patel, R. P. Patel, J. R. Lancaster Jr., V. M. Darley-Usmar, D. W. Kraus, *Anal. Biochem.*, 2005, **341**, 40.

13 N. Karbanee, R. P. van Hille, A. E. Lewis, *Ind. Eng. Chem. Res.*, 2008**,** **47**, 1596.
14 W. Xuan, C. Sheng, Y. Cao, W. He, W. Wang, *Angew. Chem. Int. Ed.*, 2012, **51**, 2282.
15 (a) H. Peng, Y. Cheng, C. Dai, A. L. King, B. L. Predmore, D. J. Lefer, B. Wang, *Angew. Chem. Int. Ed.*, 2011*,* **50***,* 9672; (b) S. Chen, Z.-j Chen, W. Ren, H.-w. Ai, *J. Am. Chem. Soc.*, 2012, **134**, 9589; (c) A. R. Lippert, E. J. New, C. J. Chang, *J. Am. Chem. Soc.*, 2011, **133**, 10078; (d) N. Gupta, S. I. Reja, V. Bhalla, M. Gupta, G. Kaur, M. Kumar, *Chem. Commun.*, 2015, **51**, 10875; (e) J. Cheng, J. Song, H. Niu, J. Tang, D. Zhang, Y. Zhao, Y. Ye, *New. J. Chem.*, 2016, **40**, 6384; (f) K. Renault, P.-Y. Renard, C. Sabot, *New J. Chem.*, 2017, **41**, 10432; (g) L. Yang, Y. Su, Z. Sha, Y. Geng, F. Qi, X. Song, *Org. Biomol. Chem.*, 2018, **16**, 1150; (h) Z. Qiao, H. Zhang, K. Wang, Y. Zhang, *Talanta*, 2019, **195**, 850.
16 (a) C. Liu, B. Peng, S. Li, C.-M. Park, A. R. Whorton, M. Xian, *Org. Lett.*, 2012, **14**, 2184; (b) C. Liu, J. Pan, S. Li, Y. Zhao, L. Y. Wu, C. E. Berkman, A. R. Whorton, M. Xian, *Angew. Chem. Int. Ed.*, 2011, **123**, 10327.
17 (a) K. Sasakura, K. Hanaoka, N. Shibuya, Y. Mikami, Y. Kimura, T. Komatsu, T. Ueno, T. Terai, H. Kimura, T. Nagano, *J. Am. Chem. Soc.*, 2011, **133**, 18003; (b) X. Yao, Y.-Y. Guo, J.-X. Ru, C. Xu, Y.-M. Liu, W.-W. Qin, G.-L. Zhang, X.-L. Tang, W.-S. Liu, *Sens. Actuators B*, 2014, **198**, 20.
18 (a) K. Renault, C. Sabot, P.-Y. Renard, *Eur. J. Org. Chem.*, 2015, 7992; (b) X. Xie, C. Yin, Y. Yue, J. Chao, F. Huo, *Sens. Actuators B Chem.* 2018, **277**, 647; (c) L.-L. Zhang, H.-K. Zhu, C.-C. Zhao, X.-F. Gu, *Chin. Chem. Lett.*, 2017, **28**, 218. (d) G. Li, S. Ma, J. Tang, Y. Ye, *New J. Chem.*, 2019, **43**, 1267. (e) H. Niu, B. Ni, K. Chen, X. Yang, W. Cao, Y. Ye, Y. Zhao, *Talanta*, 2019, **196**, 145.
19 (a) B. Wang, P. Li, F. Yu, P. Song, X. Sun, S. Yang, Z. Lou, K. Han, *Chem. Commun.*, 2013, **49**, 1014; (b) Z. Lou, P. Li, Q. Pan, K. Han, *Chem. Commun.*, 2013, **49**, 2445; (c) B. Wang, P. Li, F. Yu, J. Chen, Z. Qu, K. Han, *Chem. Commun.*, 2013, **49**, 5790. Z. Lou, P. Li, K. Han, *Methods Mol. Biol.* 2015, **1208**, 97.
20 (a) L. Zhang-Rong, L. Peng, H. Ke-Li, *Acta Phys.-Chim. Sin.*, 2017, **33**, 1573; (b) X. Jiang, L. Wang, S. L. Carroll, J. Chen, M. C. Wang, J. Wang, *Antioxid. Redox Signal.*, 2018, **29**, 518.
21 (a) B. Halliwell, M. Whiteman, *Br. J. Pharmacol.*, 2004, **142**, 231; (b) B. Halliwell, *Trends Biochem. Sci.*, 2006, **31**, 509.
22 (a) D. Oushiki, H. Kojima, T. Terai, M. Arita,, K. Hanaoka, Y. Urano, T. Nagano, *J. Am. Chem. Soc.*, 2010, **132**, 2795; (b) K. Cui, D. Zhang, G. Zhang, D. Zhu, *Tetrahedron Lett.*, 2010, **51**, 6052; (c) A. V. Bizyukin, L. G. Korkina, B. T. Velichkovskii, *Bull. Exp. Biol. Med.*, 1995, **119**, 347; for a review, see (d) A. Gomes, E. Fernandes, J. L. F. C. Lima, *J. Biochem. Biophys. Methods*, 2005, **65**, 45.
23 (a) E. A. Podrez, H. A. Abu-Soud, S. L. Hazen, *Free Radical Biol. Med.*, 2000, **28**, 1717; (b) D. I. Pattison, M. J. Davies, *Chem. Res. Toxicol.*, 2001, **14**, 1453; (c) D. I. Pattison, M. J. Davies, *Biochemistry*, 2006, **45**, 8152.
24 A. Ishii, Y. Yamaguchi, N. Nakata, *Org. Lett.*, 2011, **13**, 3702.
25 (a) Z. Lou, P. Li, K. Han, *Acc. Chem. Res.*, 2015, **48**, 1358; (b) D. Wu, L. Chen. N. Kwon, J. Yoon, *Chem* 2016, **1**, 674; see also (c) D. Escudero, *Acc. Chem. Res.*, 2016, **49**, 1816.
26 T. M. Swager, O. Haze, *Synfacts*, 2011, **10**, 1067.
27 (a) A. Ishii, T. Annaka, N. Nakata, *Chem. Eur. J.*, 2012, **18**, 6428; (b) A. Ishii, N. Nakata, *J. Synth. Org. Chem. Jpn.*, 2018, **76**, 1042.
28 (a) F. Yu, P. Li, P. Song, B. Wang, J. Zhao, K. Han, *Chem. Commun.*, 2012, **48**, 4980; (b) E. W. Miller, S. X. Bian, C. J. Chang, *J. Am. Chem. Soc.*, 2007, **129**, 3458; (c) Y. Yamada, Y. Tomiyama, A. Morita, M. Ikekita, S. Aoki, *ChemBioChem*, 2008, **9**, 853; (c) F. Yu, P. Li, G. Li, G. Zhao, T. Chu, K. Han, *J. Am. Chem. Soc.*, 2011, **133**, 11030; (d) Y. Koide, M. Kawaguchi, Y. Urano, K. Hanaoka, T. Komatsu, M. Abo, T. Terai, T. Nagano, *Chem. Commun.*, 2012, **48**, 3091; see also (e) F. Yu, P. Li, B. Wang, K. Han, *J. Am. Chem. Soc.,* 2013, **135**, 7674.
29 (a) Q. Yu, K. Y. Zhang, H. Liang, Q. Zhao, T. Yang, S. Liu, C. Zhang, Z. Shi, W. Xu, W. Huang, *ACS Appl. Mater. Interfaces*, 2015, **7**, 5462; (b) B. Wang, N. Jiang, W. Sun, Q. Wang, G. Zheng, *RSC Adv.*, 2016, **6**, 36906.
30 Y. Yuan, M. H. Knaggs, L. B. Poole, J. S. Fetrow, F. R. Salsbury Jr., *J. Biomol. Struct. Dyn.*, 2010, **28**, 51.
31 (a) T. G. Back, Z. Moussa, M. Parves, *Angew. Chem. Int. Ed.*, 2004, **43**, 1268; (b) D. J. Press, N. M. McNeil, A. Rauk, T. G. Back, *J. Org. Chem.*, 2012, **77**, 9268; (c) D. J. Press, T. G. Back, *Can. J. Chem.*, 2016, **94**, 305; (d) N. M. R. McNeil, D. J. Press, D. M. Mayder, P. Garnica, L. M. Doyle, T. G. Back, *J. Org. Chem.*, 2016, **81**, 7884.
32 (a) M. Iwaoka, F. Kumakura, M. Yoneda, T. Nakahara, K. Henmi, H. Aonuma, H. Nakatani, S. Tomoda, *J. Biochem.*, 2008, **144**, 121; (b) K. Arai, K. Dedachi, M. Iwaoka, *Chem. Eur. J.*, 2011, **17**, 481.
33 E. A. Cowan, C. D. Oldham, S. W. May, *Arch. Biochem. Biophys.*, 2011, **506**, 201.
34 S. Antony, C. A. Bayse, *Inorg. Chem.*, 2011, **50**, 12075.
35 R. Steudel, *Top. Curr. Chem.*, 2003, **231**, 99.
36 G. M. Sheldrick, *Acta Cryst.,* 2008, **A64**, 112.
37 R. M. Uppu, *Anal. Biochem.*, 2006, **354**, 165.
38 Gaussian 09, Revision D.01, M. J. Frisch, G. W. Trucks, H. B. Schlegel, G. E. Scuseria, M. A. Robb, J. R. Cheeseman, G. Scalmani, V. Barone, B. Mennucci, G. A. Petersson, H. Nakatsuji, M. Caricato, X. Li, H. P. Hratchian, A. F. Izmaylov, J. Bloino, G. Zheng, J. L. Sonnenberg, M. Hada, M. Ehara, K. Toyota, R. Fukuda, J. Hasegawa, M. Ishida, T. Nakajima, Y. Honda, O. Kitao, H. Nakai, T. Vreven, J. A. Montgomery, Jr., J. E. Peralta, F. Ogliaro, M. Bearpark, J. J. Heyd, E. Brothers, K. N. Kudin, V. N. Staroverov, T. Keith, R. Kobayashi, J. Normand, K. Raghavachari, A. Rendell, J. C. Burant, S. S. Iyengar, J. Tomasi, M. Cossi, N. Rega, J. M. Millam, M. Klene, J. E. Knox, J. B. Cross, V. Bakken, C. Adamo, J. Jaramillo, R. Gomperts, R. E. Stratmann, O. Yazyev, A. J. Austin, R. Cammi, C. Pomelli, J. W. Ochterski, R. L. Martin, K. Morokuma, V. G. Zakrzewski, G. A. Voth, P. Salvador, J. J. Dannenberg, S. Dapprich, A. D. Daniels, O. Farkas, J. B. Foresman, J. V. Ortiz, J. Cioslowski, and D. J. Fox, Gaussian, Inc., Wallingford CT, 2013.
39 (a) J. P. Perdew, M. Ernzerhof, K. Burke, *J. Chem. Phys.*, 1996, **105**, 9982; (b) C. Adamo, V. Barone, *J. Chem. Phys.*, 1999, **110**, 6158.
40 (a) D. Jacquemin, J. Preat, V. Wathelet, M. Fontaine, E. A. Perpète, *J. Am. Chem. Soc.*, 2006, **128**, 2027; (b) F. Cervantes-Navarro, D. Glossman-Minik, *J. Mex. Chem. Soc.*, 2013, **57**, 19.

Upon treatment with H_2S in MeCN-PBS, the fluorescence dormant selenoxides of dibenzobarrelene- and benzobarrelene-based 1-seleno-1,3-butadiene derivatives are rapidly converted to the strongly fluorescent selenides.